On the Interpolation of Eigenvalues and a Resultant Integration Scheme*

D. D. KOELLING

*Materials Science and Technology Division,
Argonne National Laboratory, Argonne, Illinois 60439*

AND

J. H. WOOD

Los Alamos National Laboratory, Los Alamos, New Mexico 87545

The interpolation of one-electron energy band eigenvalues by way of an interpolating function expanded as a linear sum of star functions with expansion oefficients determined via a spline-like variational scheme is described. We discuss the practical aspects of such a scheme (first, set up by Shankland) and establish that it is a viable one; we then observe that it can serve as the basis of a very useful integration scheme. The viability is established through a discussion of the choice of the interpolating function and the associated problems of point set selection and truncation of the expansion. The proposed integration scheme arises from the crucial observations that the interpolation formalism can be described in terms of a transfer matrix which operates on the data to yield the expansion coefficients; this matrix depends on the choice of the variational, the point set, and the truncation but not on the data. This allows one to produce a very powerful integration scheme which is applicable to a wide class of problems. © 1986 Academic Press, Inc.

Although linearized energy band methods can rapidly determine one-electron energy eigenvalues throughout the Brillouin zone, some problems require such a dense sampling of k-points that the concomitant cost is prohibitive. Thus, a reliable interpolation scheme that converts the ab initio results obtained on a coarse k-space grid over to a tabulation on a fine grid is still a valuable software tool in the calculation of densities of states and related quantities. The earliest such scheme employed local polynomial fitting; this was subsequently improved with the use of spline concepts. This scheme is still used as the final step in integration methods, e.g., in the tetrahedron-based schemes, a local linear or quadratic interpolation is

used. However, such local fittings are cumbersome and often inadequate when employed on a global basis (i.e., throughout the Brillouin zone). An alternate set of schemes based on a Fourier (plane wave) analysis is global in nature since, in such schemes, one attempts to fit a band over the entire zone. The linear combination of atomic orbitals (LCAO) [1] and the combined interpolation schem (CIS [2] can be regarded as elaborate variants of such global Fourier schemes. However, both these methods involve nonlinear fitting and diagonalization of matrices; consequently, they are less desirable as numerical interpolation schemes and are more commonly used as models of the physical system. The most prevalent approaches to global Fourier-based interpolation involve least squares fitting, in one form or another.

Fourier function based approaches start from the observation that an energy band has the full symmetry of the crystal's reciprocal space. Thus the star functions

$$S_m(\mathbf{k}) = \frac{1}{n} \sum_{\{\alpha\}} \exp i[\alpha \mathbf{R}_m] \cdot \mathbf{k} \tag{1}$$

are a natural expansion set. The sum on α runs over all n operations of the point group of the crystal while R_m denotes a real-space lattice translation. (The phase factors encountered in expanding a real-space function for a crystal with a nonsymmorphic space group do not occur in these k-space expansions.) The factor $1/n$ forces the normalization of the function to the volume of the Brillouin zone. Note that because all the αR_m are lattice vectors, arguments of the sines and cosines encountered in evaluating $S_m(k)$ are multiples of the primitive translations; hence, all the star functions at a given k point can be evaluated from a maximum of nine sine–cosine evaluations with trigonometric identities providing the remaining information. Assuming ab initio calculated data $e(k)$ at N points, one can perform a least squares fit using M star functions

$$\tilde{e}(\mathbf{k}) \simeq \sum_{m=1}^{M} a_m S_m(\mathbf{k}), \tag{2}$$

where (for stability) M is typically less than $\frac{2}{3}$ of N. If M is chosen too large, or if the band has "difficult" structure, the agreement between the fit and the data will still be good, but the fit will exhibit wild oscillations in between the N data points; this is generally reflected in large variations over the fitting coefficients a_m. The choice $M = N$, for example, leads to such instabilities even though the ab initio data and the fitted values agree precisely at the N data points.

What is meant by "difficult" structure? The most difficult structures occur as a result of band crossings. Because a band must be defined by energy ordering, the crossing of two $e(k)$ curves results in a kink structure and such a structure is always a problem for Fourier series analysis as it leads to Gibbs ringing. Removal of such crossings by a perturbation such as the spin–orbit interaction can help but, in general, the problem does not entirely disappear. Multiple fits can also alleviate the

situation but this is a move away from a global fit [3]. [A prime example of a recalcitrant band is band six of a transition metal; this band is d-like (flat) near the center of the zone and plane-wave-like (parabolic) near the zone boundaries with a sharp knee (kink) in between.]

Least squares procedures lead to the fit function passing near (but, in general, not through) the N data points. This inevitably sacrifices some of the precision with which these eigenvalues were originally determined. An alternative procedure, first proposed by Shankland [4], uses more functions than points $(M > N)$. The fit is required to pass through all data points, and the additional freedom in the fit is used to suppress oscillations between points. This suppression is accomplished by minimising an auxiliary roughness functional with the choice of functional motivated by spline analyses. One seeks to minimize the roughness of a fit in much the same manner as does a draftsman employing a spline. Shankland defined this functional R (for roughness) as

$$R \equiv \sum_{i=1}^{N} \sum_{m=1}^{M} a_m^2 S_M^2(k_i)\{C_0 + C_1 |R_m|^2 + C_2 |R_m|^4 + \cdots\}, \qquad (3)$$

where the choice of the coefficients C_0, C_1, and C_2 are left to the practitioner. (This freedom or indeterminacy in defining R has been a worrisome point to many practitioners—the authors included). It is reassuring that the quality of the fit is insensitive to the choice—note that, as given, R is defined by the two parameters, say C_1/C_0 and C_2/C_0.] As discussed by Shankland, the term involving C_0 serves to minimize the roughness (maximize the smoothness) of the interpolating function $\tilde{e}$, that involving C_1 minimizes the roughness of the first derivative, and so on. In particular, the C_0 term legislates against the occurrence of large coefficients a_m of opposite sign, a situation noted for the least squares problem. Recall that this is all done under the constraint that the interpolating function $\tilde{e}$ pass through all the data points $e(k_j)$.

The superfluous C_0 can be set to unity and the roughness coefficient defined as

$$R \equiv \sum_{m=1}^{M} a_{km}^2 \rho(R_m),$$
$$\rho(R) \equiv 1 + C_1 |R|^2 + C_2 |R|^4 + \cdots. \qquad (4)$$

It is useful to reexamine the variational solution of the problem defined in the previous paragraph since information can be extracted from the various steps. The solution is based on a standard Lagrangian formulation by defining the variational quantity R^* which includes the constraints according to

$$R^* = R - 2 \sum_i \lambda_i [e(\mathbf{k}_i) - \tilde{e}(\mathbf{k}_i)]. \qquad (5)$$

The factor of 2 is inserted to simplify later expressions. The variation of this quantity with respect to the λ parameter returns the Eqs. (2) with $k = k_i$ and $\tilde{e}$ replaced

by e. These equations are simply the requirement that the fit pass through the data. Variation with respect to the a_m,

$$\frac{\partial R^*}{\partial a_m} = 2\left[a_m \rho(R_m) - \sum_{i=1}^{N} \lambda_i S_m(k_i)\right] = 0 \tag{6}$$

relates the λ parameters to the data points $e(k_j)$ according to

$$e(k_j) = \sum_{i=j}^{N} H_{ji}\lambda_i,$$
$$H_{ji} = \sum_{m=1}^{M} S_m(k_j) S_m(k_i)/\rho(R_m). \tag{7}$$

It is instructive to consider the special case $\rho(R) = 1$. If a complete set of Fourier functions S_m were to be used, H_{ji} would be a delta function with argument $(k_j - k_i)$ and the λ_i would equal the original data $e(k_i)$. Consequently, one expects the actual H_{ji} to be fairly local in $|k_j - k_i|$ and λ_i to be close to $e(k_i)$. Inclusion of the higher terms in $\rho(R)$ will tend to delocalize H_{ji} because the influence of the short wavelength (large m) S_m terms will be reduced. We have examined this by plotting $G_{ij} \equiv H_{ij}^2/(H_{ii}H_{jj})$ as a function of the distance between k_i and k_j.

The inverse of the matrix H is utilized to solve Eq. (7) for λ_i. Equation (6) then yields

$$a_m = \sum_{j=1}^{N} T_{mj}e(k_j),$$
$$T_{mj} = \sum_{i=1}^{N} S_m(k_i) H_{ij}^{-1}/\rho(R_m). \tag{8}$$

Given the a_m, one has a solution which generates a representation of the band. Note that T does not depend on $e(\mathbf{k})$ but merely on the roughness function, star functions used, and choice of sampling points. Thus one has a linear mapping of the data into the chosen representation.

This representation can then be used to develop an interpolation formula for any given point in the Brillouin zone. One then obtains

$$e(\mathbf{k}) = \sum_{j=1}^{N} J(k, k_j) e(k_j),$$
$$J(k, k_j) = \sum_{m=1}^{M} S_m(k) T_{mj} = \sum_{mj} \frac{S_m(k_i) S_m(k)}{\rho_m(R_m)} H_{ij}^{-1}, \tag{9}$$

as the desired interpolation formula. Because an interpolation formula is obtained, it will be wise to obtain data $e(k_j)$ throughout the zone so that extrapolation can be avoided; generally, extrapolation performed with an interpolation formula is

fraught with risk. This form of interpolation has possibilities for the task of converting from one grid to another. We mention it for completeness but proceed using the expansion formula of Eq. (8).

One of the virtues of the present scheme is that the coefficients T and J are completely defined once one has chosen the lattice, the set of star functions S_m, and the form of the roughness function R. In choosing the latter, we rely on the general rule of thumb that employment of high order terms in a numerical scheme should be avoided unless absolutely need. This suggests retaining only the first term in R and adding the higher terms only if required. The first term already imposes a considerable constraint on oscillations in the interpolation function; as we have already argued, inclusion of the higher order terms acts to delocalize the interpolation—normally, this is not a desirable feature. There is only one argument that can be made in favor of inclusion of higher order terms and it is a very important one. Consider the case where the grid of data points k_j is a regular one. Now there will exist a real space vector R_Q such that the star function S_{m+Q} will have the same value as the star function S_m on the grid. One would wish that the algorithm would assign a coefficient of zero to this star function—in fact, the present scheme yields

$$a_{(m+Q)}/a_m = \rho(R_m)/\rho(R_m + Q) \tag{10}$$

so that the weight is removed from the higher order star function only to the extent that the associated roughness exceeds that of the lower order star function. Most desirable is that the algorithm would automatically remove such "duplicate" functions. Corrective action can be taken by shifting away from a regular grid of data points to break the equivalence. In the absence of either of these solutions, the coefficients C_1 ád C_2 in the expression for R may be used as adjusting knobs for damping out oscillations (induced by the presence of the high order star functions). If the data grid is reasonably fine, any repetition vector R_Q will be so large that the R^2 and R^4 occurring in the expression for the roughness will lead to considerable damping of a_{m+Q} relative to a_m; this will be true even when C_1 and C_2 are chosen rather small. Tests indicate that the results are fairly insensitive to the actual values of C_1 and C_2 so long as they are nonzero. Thus, plots of the spread of H with respect to $(k_i - k_j)$ show that the width of H increases when C_1 and C_2 are set to nonzero; however, this width is fairly insensitive to their actual values. Actually, one is more interested in the behavior of H^{-1} than that of H because it is the inverse that occurs in the interpolation equations (Eqs. (8) and (9)). We find that the width of this quantity to be far less sensitive to the particular values of C_1 and C_2 than is H itself.

The free electron bands can be used as a most informative example. A test data base is formed by tabulating the first ten bands for an *fcc* crystal on a $\pi/4a$ cubic mesh. This yields an equally spaced mesh of $N = 85$ inequivalent points. It will be seen that the mesh could be improved upon but that is not consistent with our purpose here. Two truncations were used based on $|R|$. The smaller included all stars
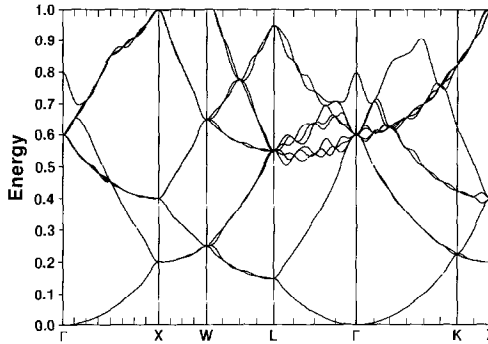
FIG. 1. Fit to the free electron bands. This figures demonstrates both the stengths and the break-down modes of the method as discussed in the text. Tick marks show the position of the actual data.

for $|R| \leqslant 8\pi \sqrt{3}/a$ amounting to $M = 165$ star functions in the expansion set. The larger for $|R| \leqslant 10\pi \sqrt{3}/a$ had $M = 306$ star functions in the expansion set. Finally, to remove a dependence on lattice constant, C_1 and C_2 were renormalized by R_1^{-2} and R_1^{-4} where R_1 is the nearest neighbor distance. Fits were then performed first for $C_1 = C_2 = 0$ and then for varying values between zero and one. These fits were then examined by plotting the resultant interpolation, by looking at the size of the maximum coefficient, and by looking at the root mean square of the coefficients. For the smaller function set, these last two checks revealed very little for all variations of the C_1 and C_2. The case $C_1 = C_2 = 0$ graphically showed some oscillations between the data points but these rapidly reduced as additional smoothing was turned on through either C_1 or C_2 or both. In Fig. 1, we show the representation of the bands obtained with $C_1 = C_2 = 1$. As is seen, the representation of the bottom band is quite good. Between the data points, the representation oscillates for the upper band. This is greatly reduced by going to an irregular sampling grid but, again, that is not the point of this set of experiments. The free electron bands are a very severe test case for this procedure as they exhibit many band crossings (cusps) in the Brillouin zone thus driving the Gibbs-ringing-like problem. This is precisely why the lowest band is best represented. Some such oscillation must unfortunately be tolerated if there is a band crossing. If the point sampling is made too fine for a given number of functions, the matrix H will become singular. This will occur even when only a very few pairs occur with a separation too small for the number of star functions. Using the larger set of functions $(M = 306)$, we can observe the effect of extending the expansion set. For the case $C_1 = C_2 = 1$, the two representations of these bands are indistinguishable. *However*, when the extra restraints are turned off $(C_1 = C_2 = 0)$, the situation is much worse with the larger number of functions! The maximum size and the r.m.s. size of the coefficients indicate wild oscillations which are seen in the plots (not shown) even though the data points are still fit exactly. The larger number of functions has generated many more repeating vectors for the regular grid. The

choice $C_1 = 0.1$ and $C_2 = 0$ already drops the maximum and r.m.s. coefficients to values very close to their values for $C_1 = 1$, $C_2 = 1$. Any further variation for $C_1 \geqslant 0.5$ is really indistinguishable by all three indices. It is pleasing to see this very clear demonstration of the correctness of our interpretation of the significance of the coefficients C_1 and C_2.

As a second more realistic example can be useful, the method has also been employed to represent the bands of the low symmetry material α-uranium. In this case, determination of the ab initio band calculation points is expensive so it is desirable to keep their number to a minimum. The data (band calculations) were obtained on a fairly random set so the question of the effects of a regular mesh is not relevant. The size of the maximum coefficient a_m (Eq. (2)) and the root mean square of these coefficients again serve as a measure of the smoothness and the variability of the fit. These quantities were quite stable with changes in C_1 and C_2—the maximum coefficient suffers changes in the second significant figure for C_1 and C_2 varying between 0.1 and 1.0. Again, the most remarkable feature is the stability of H^{-1} qualitatively observed in printer plots of G_{ij} defined in the same way as for H above. This supports the conclusion that the choice of the exact form of the roughness functional is not critical. While one might conceivably tailor it to a better form than that of Eq. (4), this is not a particularly pressing problem within the present methodology. This is simply a result of the dominance of the data and of the fact that any repetition vector has a much larger length than the original.

It is significant that the necessity of determining the inverse of H partially dictates the selection of the data points k_j and the truncation of the expansion of the star functions. Clearly, if any two points are identical—or equivalent—H will be singular. Similarly, if the expansion set is not sufficient to distinguish between inequivalent data points (vide supra). H will again be singular. [One could presumably obtain solutions by techniques other than those embodied in Eqs. (8) but that would involve the use of superfluous data.] Our trial experience with $\alpha - U$ provided us with concrete examples of both points. It also demonstrated that inclusion of the additional (above and beyond N) star functions does indeed provide the desired smoothness. For example, the bands along the line connecting the center of the upper face (A) of the Brillouin zone to the (011) edge (L) are
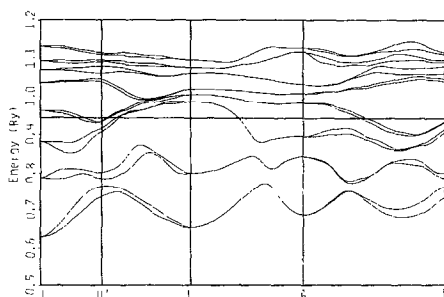

Fig. 2.   Energy bands of alpha uranium as represented by this method.

doubly degenerate. When we used 277 star functions with 141 data points, the fitted bands oscillated noticeably about one another along this line. Using 505 star functions with 149 data points (4 of the additional 8 were on that line), we found that we could not distinguish the curve on a line plotter. In the latter case, the bands were also noticeably smoother with anti-crossings and band interactions clearly discernible. We show this upper plane of the Brillouin zone in Fig. 2.

Although our initial interest in the present formalism was concerned with representing band for density-of-states and Fermi surface studies, the structure of Eqs. (8) and (9) suggests another application which may be of greater significance than is the interpolation scheme. Note that these equations relate the eigenvalue data to the star function expansion coefficients through the transfer matrix T. It is very significant that T contains no information about the data; it is determined solely by the choice of the roughness functional, tha data point set (the k_j), and the truncation of the expansion (at M functions). Thus, in carrying out an integration over the Brillouin zone, one can choose to expand the integrand in star functions and perform the integration (over the various star functions) analytically in much the same way that one carries out a Simpson's integration by expanding in a quadratic and integrating. The expansion then yields a set of points and appropriate weights for the desired integral. This process need be carried out but once for a given crystal structure and should give a very efficient sampling (which need not be regular). It should handle structure in the integrand more accurately than schemes based on Gaussian quadrature. It can even handle sharp cutoffs if they can be included in the integration rather than in the fitting process.

It is interesting to ask why one gets this clean separation of the data from the fitting coefficients when it does not obtain in the least squares procedure. Here, the data appears only in the linear constraint part of the variational function Eq. (5) with the smoothness requirement appearing in the quadratic component. The least squares treatment on the other hand, puts the data in the quadratic part inasmuch as it is the square of the deviation of the fit from the data that is being minimized. This feature mixes the data with the fitting functions and produces the non-separable form.

The utility of this observation of a resulting integration scheme is best emphasized by a significant example. Consider the calculation of the matrix elements appearing in a band calculation

$$H_{ij} = \int d^3\vec{r}\phi_i^* H\phi_j, \tag{10a}$$

$$S_{ij} = \int d^3\vec{r}\phi_i^* \phi_j. \tag{10b}$$

Since these equations are for real space, the star functions of Eq. (2) must be the real-space counterparts and reflect any nonsymmorphic character of the crystal. Otherwise, the formalism can be applied directly to any desired quantity in real

space. One must obtain the fully symmetric projection of the integrands in Eq. (10).
When this is done, one has an expansion of the integrand which can then be
analytically integrated (yielding only the $K = 0$ term). Such a technique would be
quite practical for a pseudopotential where the sharp structure near the nuclei of an
atomic site has been removed. Such an integration scheme was tested for the
overlap of LCAO-type lattice sums of Gaussian functions centered on different sites
(in a cubic lattice) since the result can also easily be obtained analytically. We then
proceeded to examine the precision of the result as we varied the Gaussian range
parameter (and thus the degree of structure in the integrand), the point set, and the
choice of smoothness parameters. What we found was that the integration was
stably quite precise (six digits) under all conditions until one exceeded sensible
bounds. For example, the error crept into the third significant figure if one's
sampling points became as far apart as one of the Gaussian range parameters. The
failure was quite graceful, however. The one case where the failure was not graceful
was where the fitting functions did not have the proper symmetry. We simulated
such a case by using fitting functions with a repetition length twice that of our lat-
tice. In that case, the scheme failed dramatically. The numbers had the correct trend
with varying $\mathbf{k}$ but barely achieved single digit precision. From our rather extensive
testing of this simple case, we concluded that this integration scheme works
extremely well so long as (1) the star functions have the appropriate symmetry, (2)
the point sampling is sufficiently dense to resolve the integrand (but the failure
mode is quite graceful), (3) the shortest wavelength (maximum K) must also be
short enough to resolve the structure but this must be satisfied if the point sampling
is adequate or the weight generation will not succeed due to the singular matrix.

The technique cannot be used without modification for an all electron calculation
because the sharp structure of the atomic site would demand the inclusion of too
many star functions and sample points. For an all electron calculation, it is attrac-
tive to utilize augmentation. Then one draws spheres around each atomic site and
treats the interior of those spheres numerically in the same way as is currently done
for the APW or KKR method. The boundary matching problem becomes a second
quite tractible numerical problem which is not discussed here. Now, the integration
is to be performed in the incomplete (interstitial) space. But, as this is to be done
analytically, it is easily accomplished. The result is

$$I = \sum_{j=1}^{N} \sum_{m=1}^{M} \langle S_m \rangle \, T_{mj} \chi(r_j) \equiv \sum_j \omega_j \chi(r_j), \tag{11}$$

where $\langle S_m \rangle$ is the integral of the star function in the interstitial region. This is a
quantity well known to practitioners of the APW method. $\chi(r_j)$ is the fully sym-
metric component of the desired integrand. If the fully symmetric part is not easily
available, then the sampling must include all equivalent points so that it will be
generated numerically. Again it is to be reiterated that the integration weights do
not depend on the integrand χ but only on the sampling point set used, the
roughness function chosen, and the number of star functions used. Thus the $\{r_j, \omega_j\}$

set can be calculated and saved as a database. Finally, note that the basis set in the interstitial region need not be plane waves. However, since the manipulation of any other basis set in this incomplete space has always required transformation to plane waves to perform the requisite interstitial integrations (note the augmented STO method [5], for example), this numerical procedure offers an efficient and fexible alternative to transforming to a linear combination of APWs [6]. We are of the opinion that this may well be the most significant result of this exercise.

REFERENCES

1. J. C. SLATER AND G. F. KOSTER, *Phys. Rev.* **94**, 1498 (1954).
2. L. HODGES, H. EHRENRICH, AND N. D. LANG, *Phys. Rev.* **152**, 505 (1966); F. M. MUELLER, *Phys. Rev.* **153**, 659 (1967).
3. L. L. BOYER, *Phys. Rev. B* **19**, 2824 (1979).
4. D. G. SHANKLAND, in *Computational Methods in Band Theory*, edited by P. Marcus, J. Janak, and A. Williams (Plenum, New York, 1971), p. 362.
5. J. DAVENPORT, *Phys. Rev. B* **29**, 2896 (1984).
6. G. ARBMAN AND D. KOELLING, *Phys. Scr.* **5**, 273 (1972).